Internal Combustion Engines
I: Fundamentals and Performance Metrics

Prof. Rolf D. Reitz,
Engine Research Center,
University of Wisconsin-Madison

2018 Princeton-Combustion Institute
Summer School on Combustion
Course Length: 9 hrs

(Mon.- Wed., June 25-27)

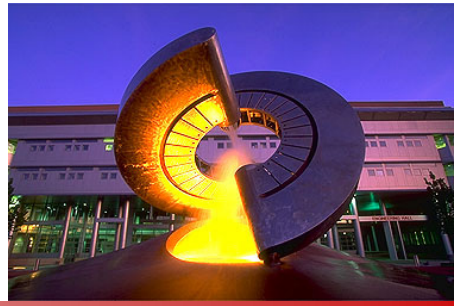

Copyright ©2018 by Rolf D. Reitz.
This material is not to be sold, reproduced or distributed without prior written permission of the owner, Rolf D. Reitz.

Short course outline:

Internal Combustion (IC) engine fundamentals and performance metrics, computer modeling supported by in-depth understanding of fundamental engine processes and detailed experiments in engine design optimization.

Day 1 (Engine fundamentals)

Hour 1: IC Engine Review, Thermodynamics and 0-D modeling
Hour 2: 1-D modeling, Charge Preparation
Hour 3: Engine Performance Metrics, 3-D flow modeling

Day 2 (Computer modeling/engine processes)

Hour 4: Engine combustion physics and chemistry
Hour 5: Premixed Charge Spark-ignited engines
Hour 6: Spray modeling

Day 3 (Engine Applications and Optimization)

Hour 7: Heat transfer and Spray Combustion Research
Hour 8: Diesel Combustion modeling
Hour 9: Optimization and Low Temperature Combustion

Diesel engine applications

On-Highway Vehicles

Marine – Propulsion or auxiliary

Power Generation – Prime power for remote locations, or standby power for edifices

Locomotive – Switchyard engines, passenger engines, European light freight

Off-Highway Vehicles – Mine trucks (haulers, loaders, etc)

Off-Highway Stationary – Petroleum industry (drill rigs, pumps, etc.)

Diesel engine applications

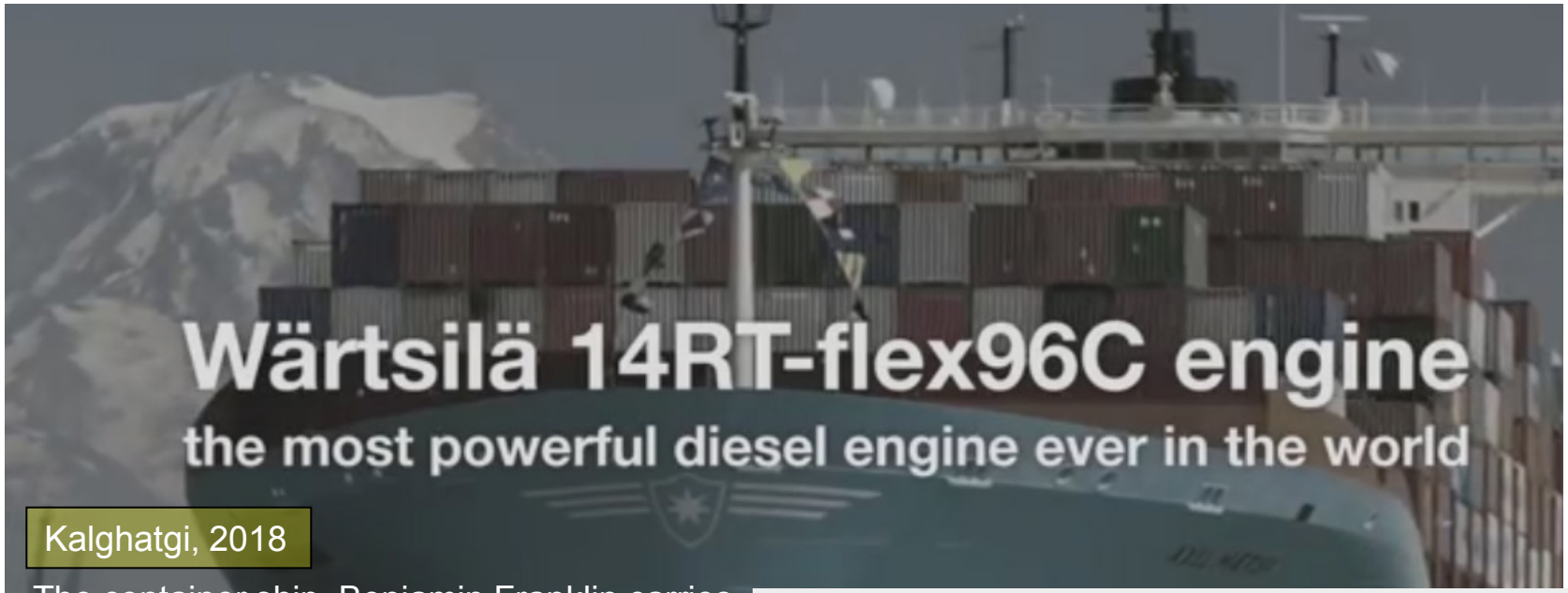

Kalghatgi, 2018

The container ship, Benjamin Franklin,carries 4.5×10^6 gals fuel (170×10^6 kWh fuel energy)
- A battery pack to hold that much energy weighs 5.8x the ship's dead weight tonnage
- Take 2 years to charge at a rate of 10 MW

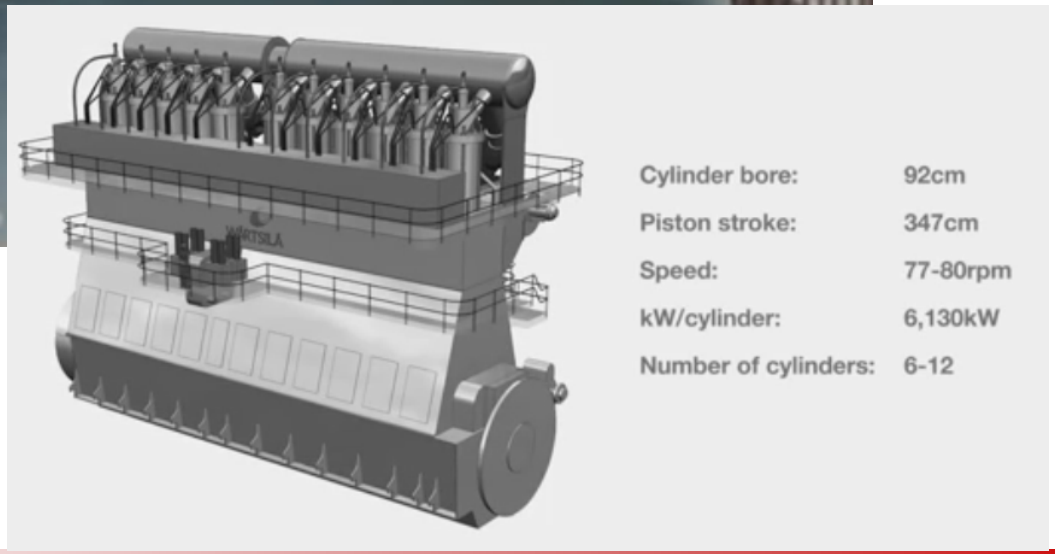

http://maniacworld.com/Worlds-Most-Powerful-Diesel-Engine.html

Diesel combustion modeling

KIVA-CHEMKIN-G code

CHEMKIN II based chemistry solver used for volumetric heat release

- Each cell considered a well-stirred reactor (WSR)
- Diesel fuel chemistry is modeled with ERC reduced n-heptane mechanism

Flame propagation considered through level set based model → G equation

Spray modeled with ERC spray models

- Gasjet theory used to reduce grid size dependency of droplet drag calculations
- Collision model considers bounce, coalescence, and fragmenting and non-fragmenting separations
- KH-RT breakup model

Tetradecane used for fuel physical properties

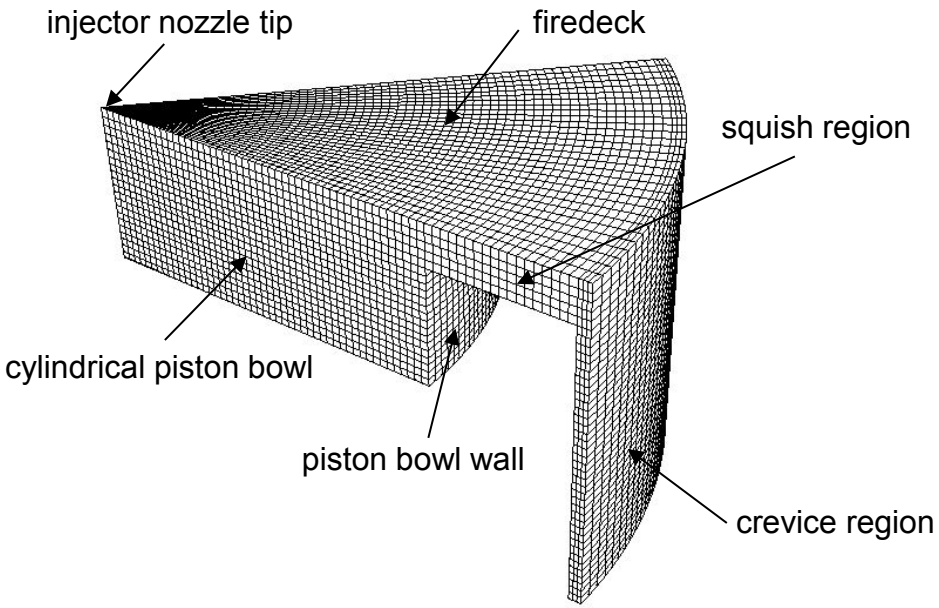

Singh, 2009

Engine setup – Sandia Cummins

Base engine type	Cummins N-14 DI diesel
Number of cylinders	1
Bore x stroke	13.97 x 15.24 cm
Connecting rod length	30.48 cm
Displacement	2.34 L
Geometric compression ratio	10.75:1
Simulated compression ratio	16:1
Bowl width	9.78 cm
Bowl depth	1.55 cm
Fuel injector type	Common-rail
Cup (tip) type	mini-sac
Number of holes	8, equally spaced
Spray included angle	152°
Nozzle orifice diameter	0.196 mm
Nozzle orifice L/D	5

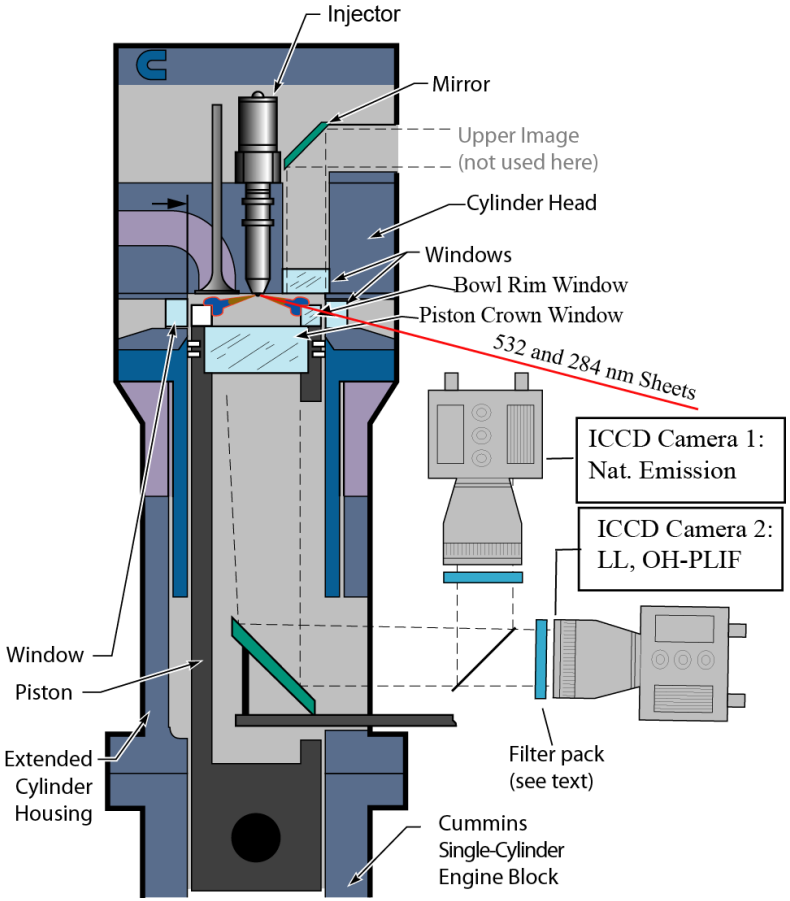

Singh, 2009

Operating conditions

Three cases ranging from Conventional to LTC diesel combustion

	HTC-short ID	HTC-med. ID	LTC-Long ID
O_2 Conc. (Vol %)	21	21	12.7
Speed (RPM)	1200	1200	1200
IMEP (bar)	4.5	4.5	3.9
Intake Temp (°C)	111	47	90
Intake Pressure (kPa)	233	192	214
TDC Motored Temperature (K)	905	800	870
TDC Motored Density (kg/m3)	24	22.3	22.9
Peak Adiabatic Flame Temp. [K]	2760	2700	2256
Rail Pressure (bar)	1200	1200	1600
Start of Injection (°ATDC)	-7	-5	-22
Duration of Injection (°CA)	10	10	7
Injection Quantity (mg)	61	61	56
Ignition Delay (°CA)	4	8.75	11
Ignition Dwell (°CA)	-6	-1.25	+4

Kokjohn, 2011

Combustion characteristics

- Simulations capture combustion characteristics accurately over a range of combustion regimes
- Results with and without consideration of flame propagation show nearly identical results

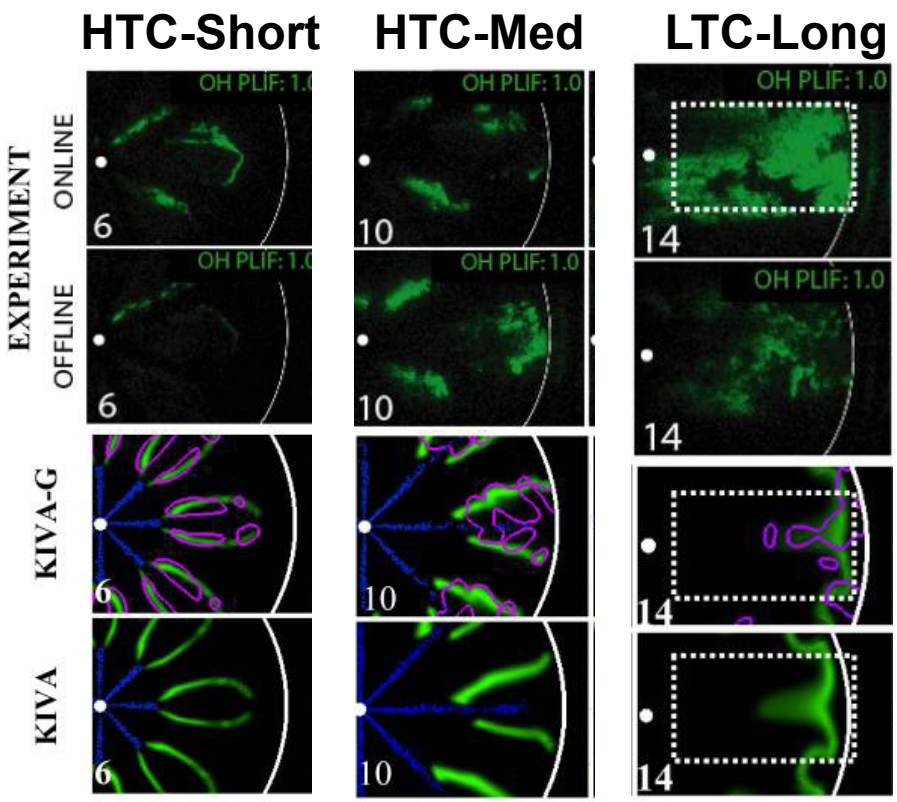

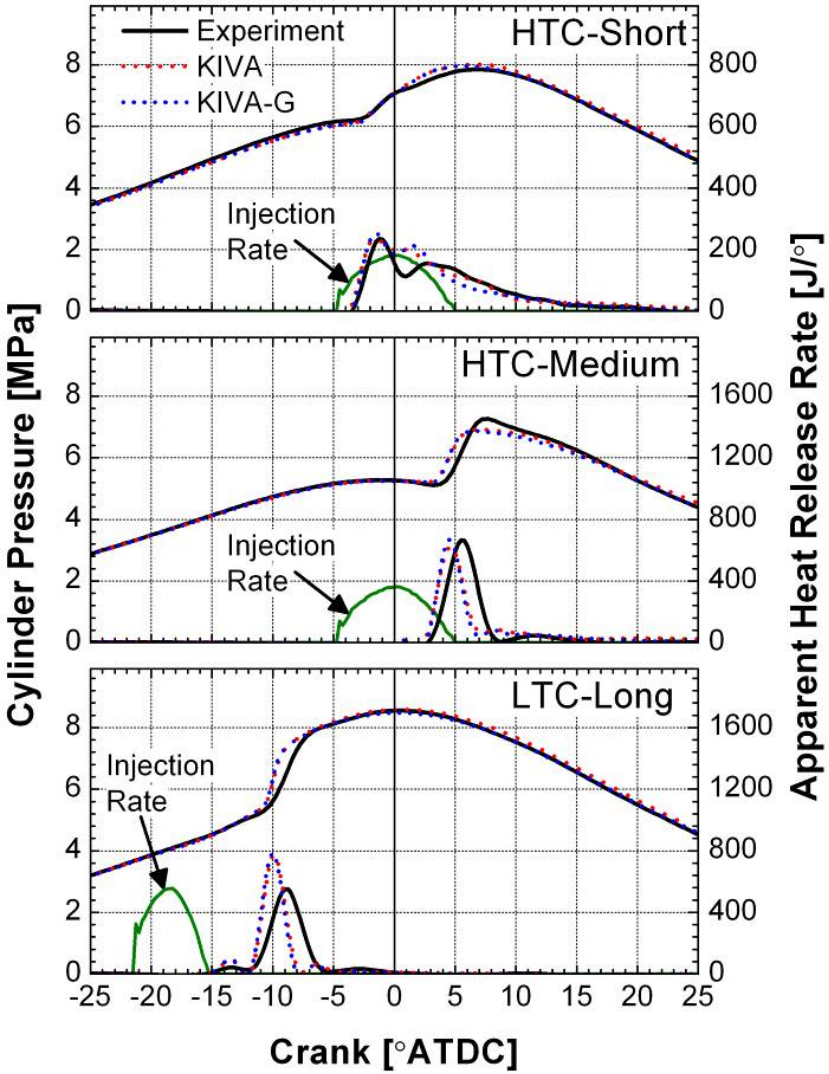

Kokjohn, 2011

Conventional diesel combustion

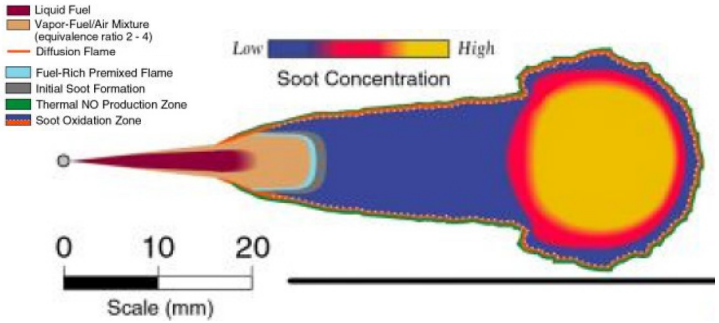

Dec's conceptual model
SAE 970873

Simulations and experiments show diffusion flame is 1 to 2 mm thick

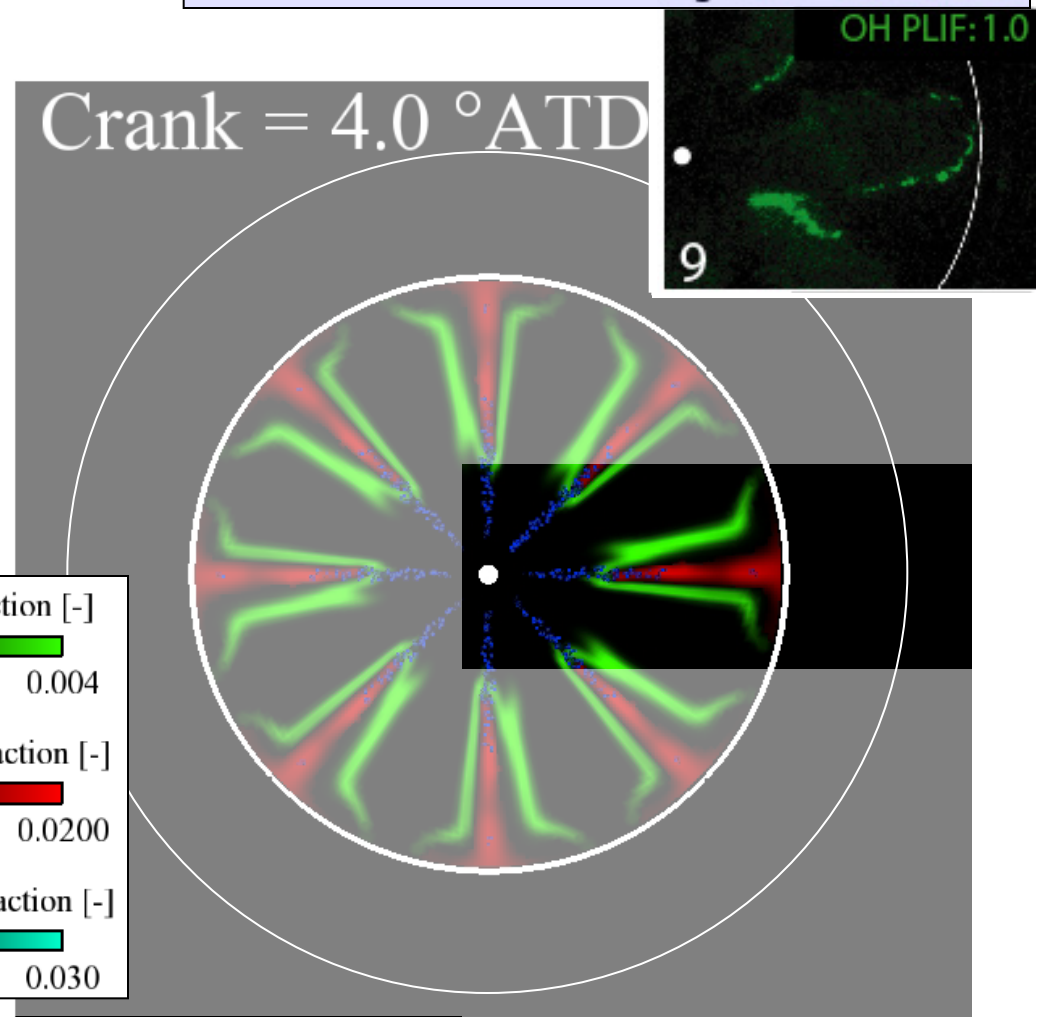

O2	21%
SOI1	-7 °ATDC
P_{inj}	1200 bar
Intake P	2.33 bar
Fuel	Diesel

Optical engine experiments
Singh, CNF 2009

Kokjohn, 2011

Conventional diesel combustion

Role of flame propagation:

Flame propagation model predicts edge or triple flame structure near lift-off location

Nose like structure with stoichiometric region closest to nozzle

Stoichiometric region shows the only non-negligible flame speed

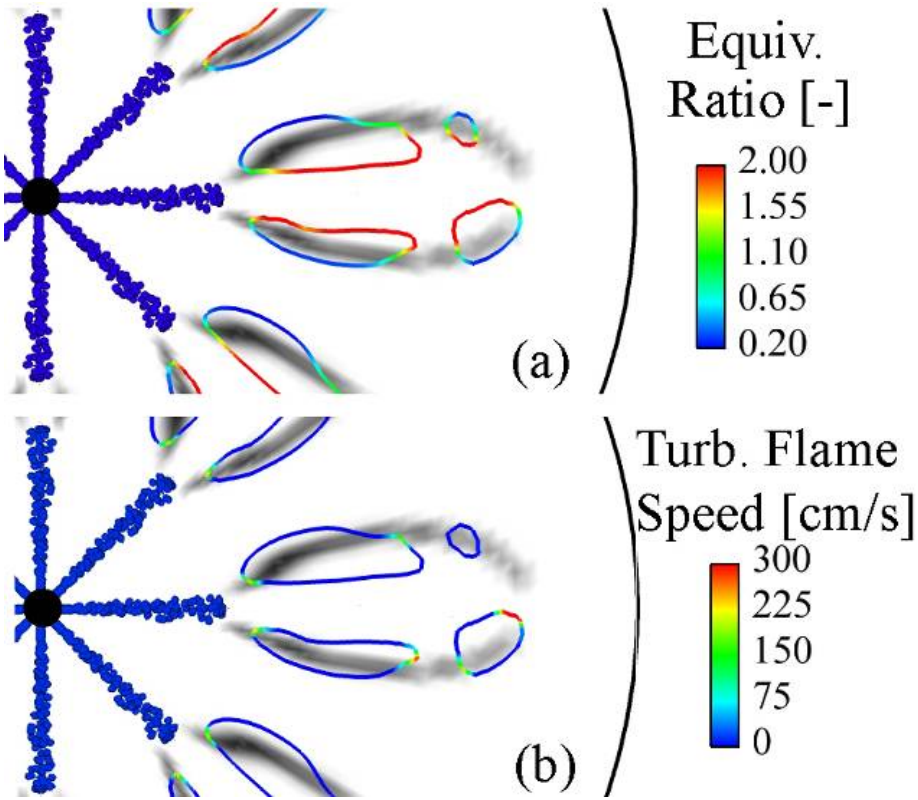

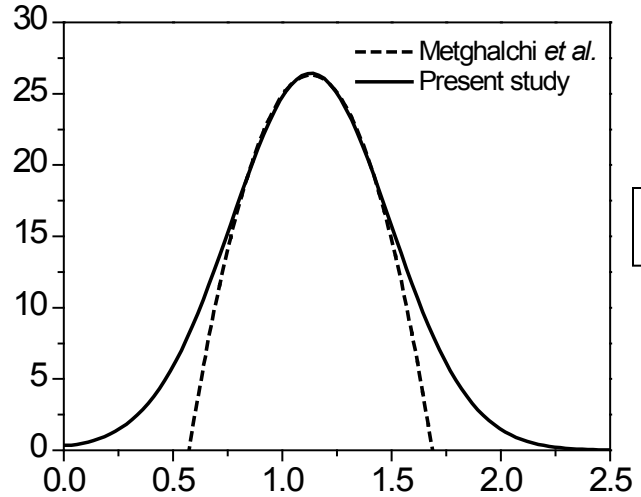

$S_T \sim S_L$

$$\frac{\partial \tilde{G}}{\partial t} + (v_f - v_{vertex}) \cdot \nabla \tilde{G} = \frac{\bar{\rho}_u}{\bar{\rho}} S_T^0 \left| \nabla \tilde{G} \right| - D_T \tilde{k} \left| \nabla \tilde{G} \right|$$

Kokjohn, 2011

LTC diesel combustion

Increased mixing time allows OH to fill jet

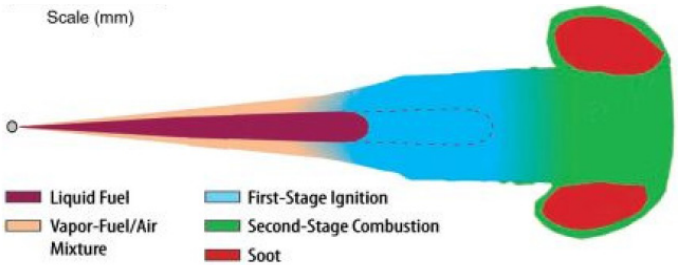

LTC conceptual model
Musculus et al.
SAE 2006-01-0079

O2	12.7%
SOI1	-22 °ATDC
P_{inj}	1600 bar
Intake P	1.92 bar
Fuel	Diesel

Optical engine experiments
Singh, CNF 2009

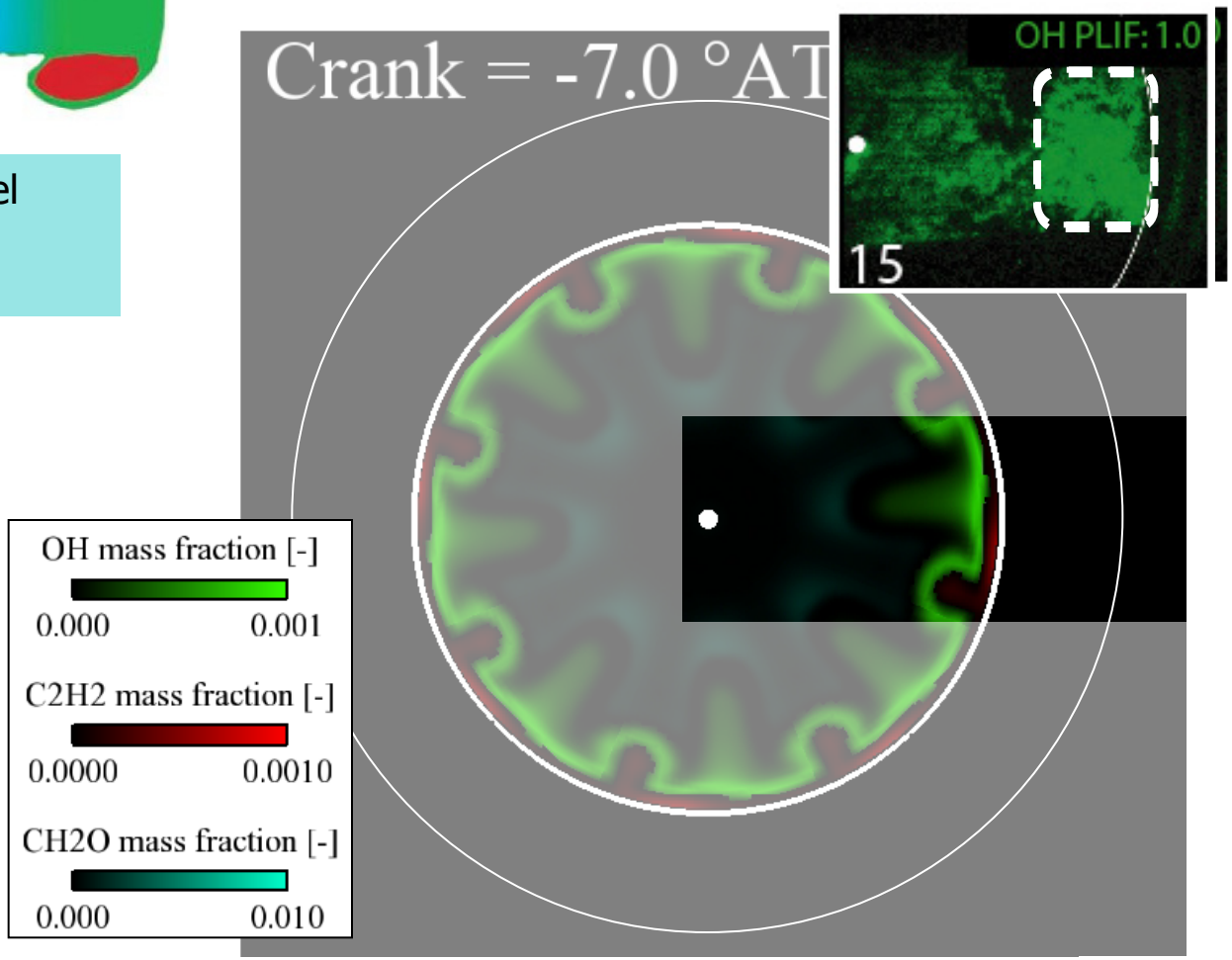

Kokjohn, 2011

Dependence of flame structure on mixing time

HTC – Short ID
- Diffusion flame is 1-2 mm thick

HTC – Medium ID
- Diffusion flame is 4 – 6 mm (exp. show 5 – 6 mm)

LTC – Early (Long ID)
- OH fills jet

Increase in reaction zone thickness with mixing time

Flame structure is captured **without** considering sub-grid scale turbulent/chemistry interactions

Ignition occurs in premixed region

Combustion is controlled by diffusion and large scale (resolved) mixing processes

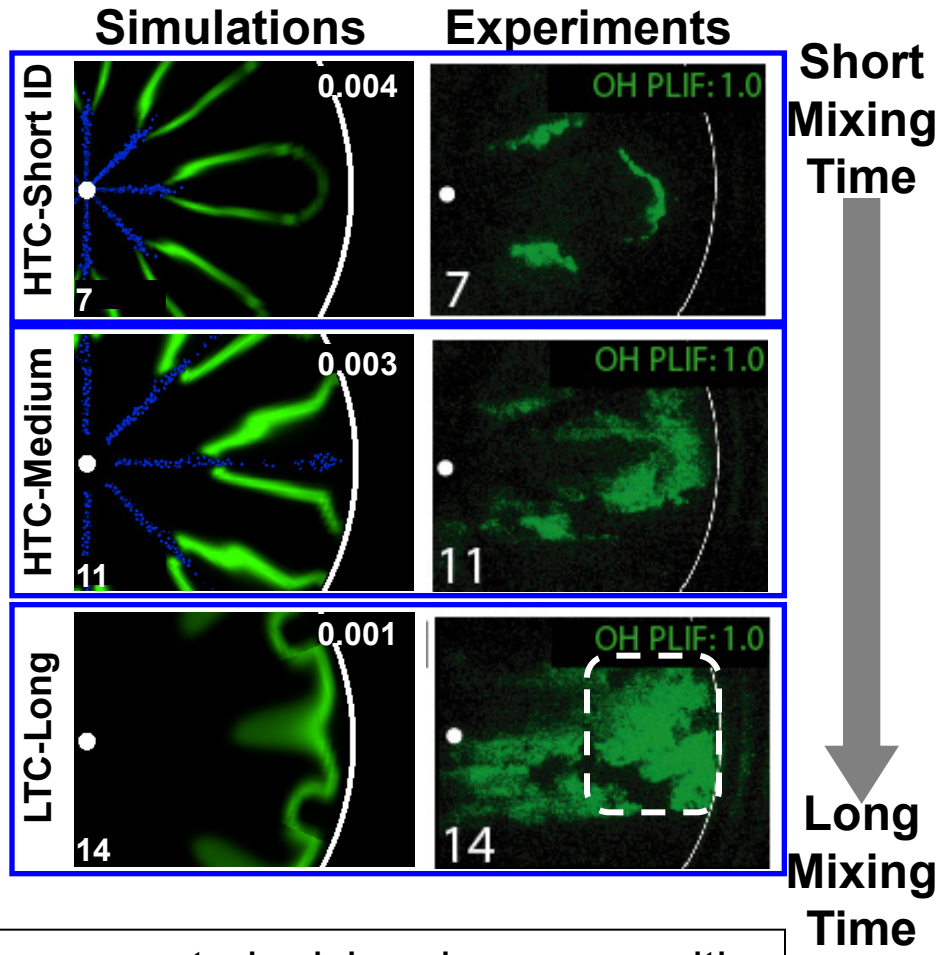

Reaction rate dependence on injection-generated mixing decreases with increasing ignition delay. If ID extends past end-of-injection, combustion-generated-mixing dominates injection-generated-mixing

Kokjohn, 2011

Singh, 2009

Flame thickness dependence on equivalence ratio

Singh et al. (2009) studied dependence of equivalence ratio on OH LIF using homogenous reactor and 1D opposed flow diffusion flame simulations

HTC-Short ID (21% O2)

OH detectable when $0.2 < \Phi < 1.6$

LTC-Long ID (12.7% O2)

OH detectable when $0.5 < \Phi < 1.2$

Kokjohn & Reitz (2011) CFD simulations show similar dependence on equivalence ratio

For a given intake oxygen concentration, OH LIF can be used to estimate local equivalence ratios

Reaction zone thickness and equivalence ratio are correlated.

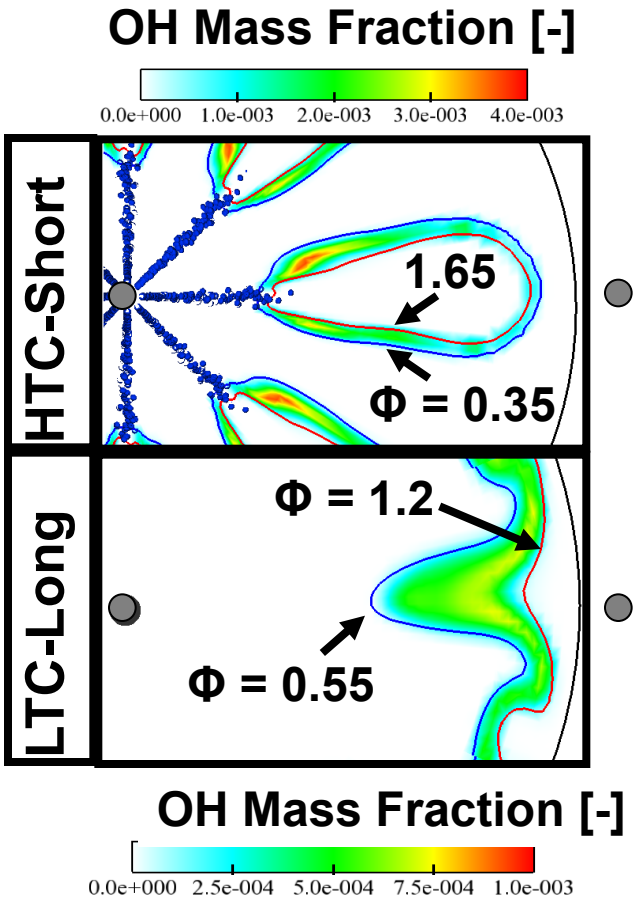

Kokjohn, 2011

Relative importance of turbulence and chemistry

HTC-Short ID

Initial reactions occur in a well mixed zone on the periphery of the jet (Φ~1)

Kinetically controlled premixed spike followed by a mixing controlled energy release

Turbulent mixing due to the injection event remains elevated during energy release

Reaction rate is controlled by the rate of transport of reactive material to the reaction zone

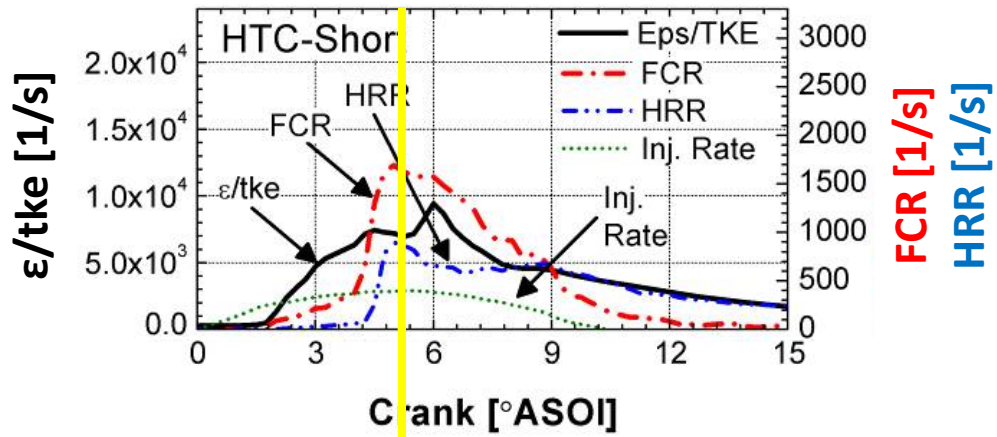

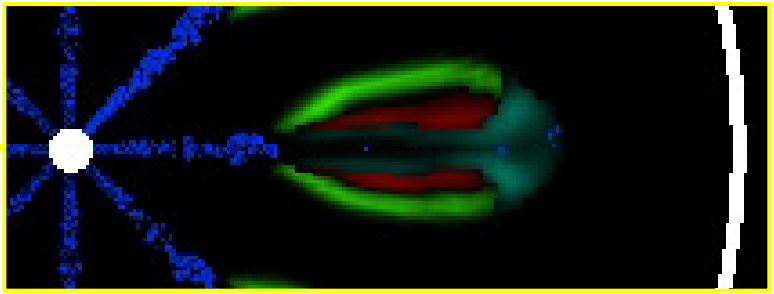

Kokjohn, 2011

Relative importance of turbulence and chemistry

HTC-Medium ID

Sharp increase in turbulent mixing rate due to injection event

Injection event is nearly complete by SOC

Turbulent mixing rate has started to decrease prior to auto-ignition

Second spike in the mixing rate due to expansion of hot products

Occurs after a significant quantity of the fuel has already been consumed

Spray induced mixing less important as ignition dwell approaches zero

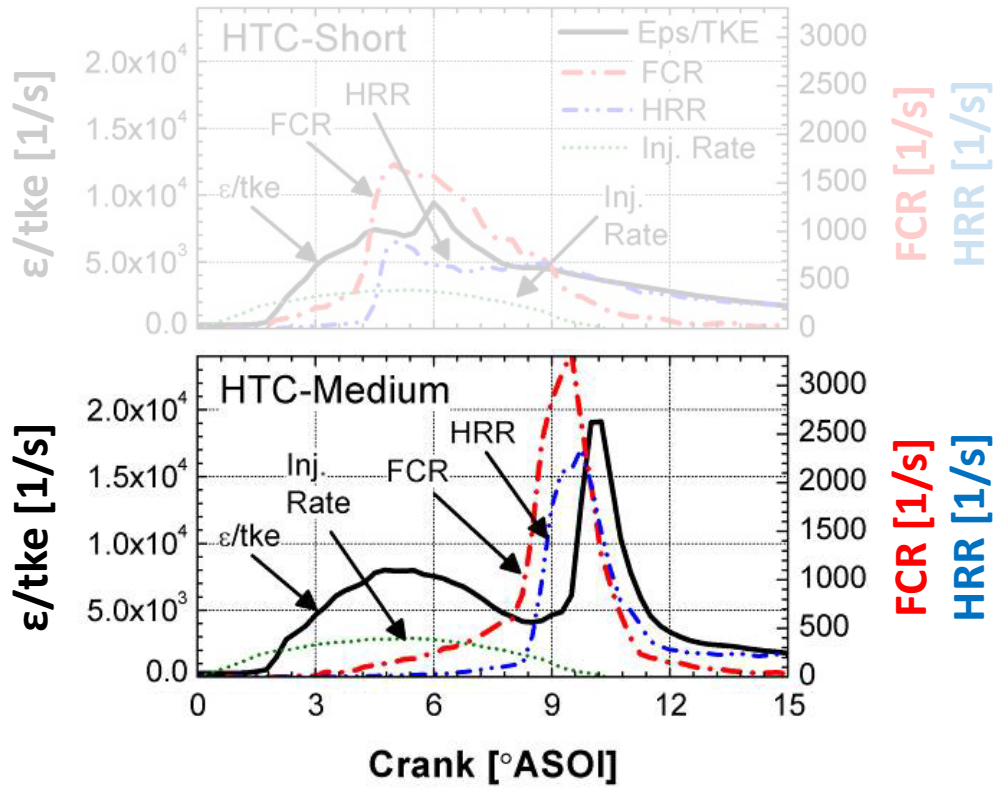

Kokjohn, 2011

Relative importance of turbulence and chemistry

LTC-Long ID

Sharp increase in turbulent mixing rate due to injection event

Injection event is completed prior to second-stage combustion

Mixing rate has dissipated nearly completely prior to auto-ignition

Fuel is consumed in two distinct stages

HR occurs rapidly and has nearly completed by the second spike in the mixing rate

Turbulent mixing appears to play a secondary role to kinetics

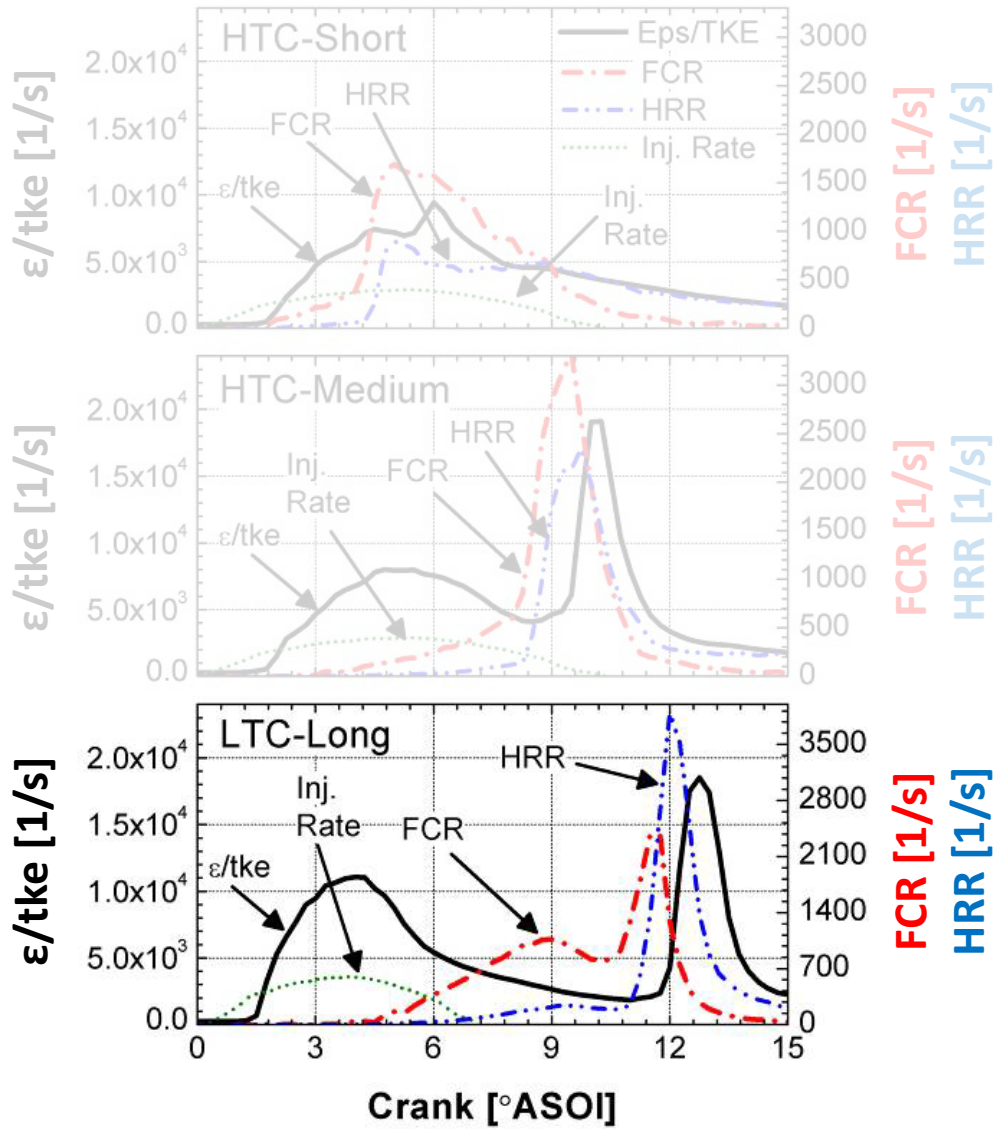

Yue, 2017

Importance of Spray Processes? Equilibrium Phase (EP) model

Recent research has shown that under diesel engine operating conditions with high injection pressures and high ambient pressures and temperatures, the spray transitions from a classical droplet dynamic- and interphase-transport-limited process into a mixing-controlled process.

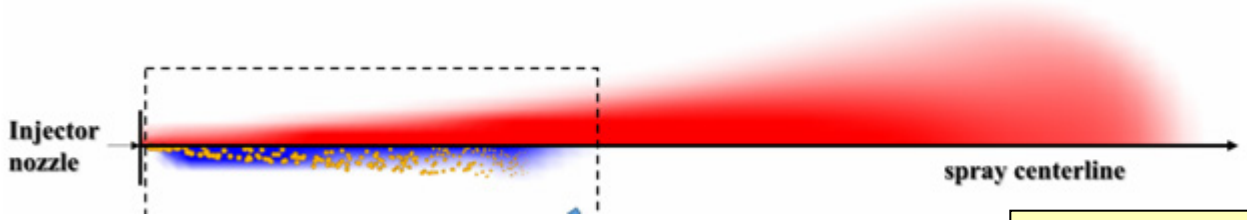

Mass flow rate of entrained ambient gas:

Siebers, 1998

$$\dot{m}_a(x) \propto \sqrt{\rho_a \cdot \rho_f} \cdot \boldsymbol{d} \cdot x \cdot \boldsymbol{U_{inj}} \cdot \tan(\theta/2) \quad (1)$$

Mass flow rate of fuel:

$$\dot{m}_f(x) \propto \rho_f \cdot \boldsymbol{d^2} \cdot \boldsymbol{U_{inj}} \quad (2)$$

a) Linear dependence of liquid length on orifice size over a wide range of conditions
b) Liquid length is insignificantly affected by injection pressure

Equilibrium Phase (EP) spray model

Siebers, 1998

Based on jet theory with the additional isothermal, non-vaporizing assumption, the axial variation of the fuel and ambient gas mass flow rates can be written as:

$$\frac{\dot{m}_f(x)}{\dot{m}_a(x)} = \frac{2}{\sqrt{1+16\tilde{x}^2}-1}, \qquad \tilde{x} = x/x^+,\ x^+ = \sqrt{\rho_f/\rho_a}\cdot\sqrt{C_a}\cdot d/\tan(\theta/2) \qquad (3)$$

At the tip of liquid length ($x = L$),

$$\frac{\dot{m}_f(L)}{\dot{m}_a(L)} = B(T_a, P_a, T_f) \qquad (4$$

$B(T_a, P_a, T_f)$ is the ratio of injected fuel and entrained ambient gas at equilibrium;

Combining Equations (3) and (4), the dimensional liquid length is:

$$L = C_L \cdot \frac{\sqrt{C_a}\cdot d}{\tan(\theta/2)} \cdot \sqrt{\frac{\rho_f}{\rho_a}} \sqrt{\left(\frac{2}{B(T_a,P_a,T_f)} + 1\right)^2 - 1} \qquad (5)$$

Yue, 2017

Equilibrium Phase (EP) spray model

In the EP model the liquid is injected into the computational domain as Lagrangian parcels, as in the LDEF approach, then released to an Eulerian liquid phase

Lagrangian liquid $\xrightarrow{\text{release}}$ Eulerian liquid $\xleftrightarrow{\text{local equilibrium}}$ Eulerian vapor

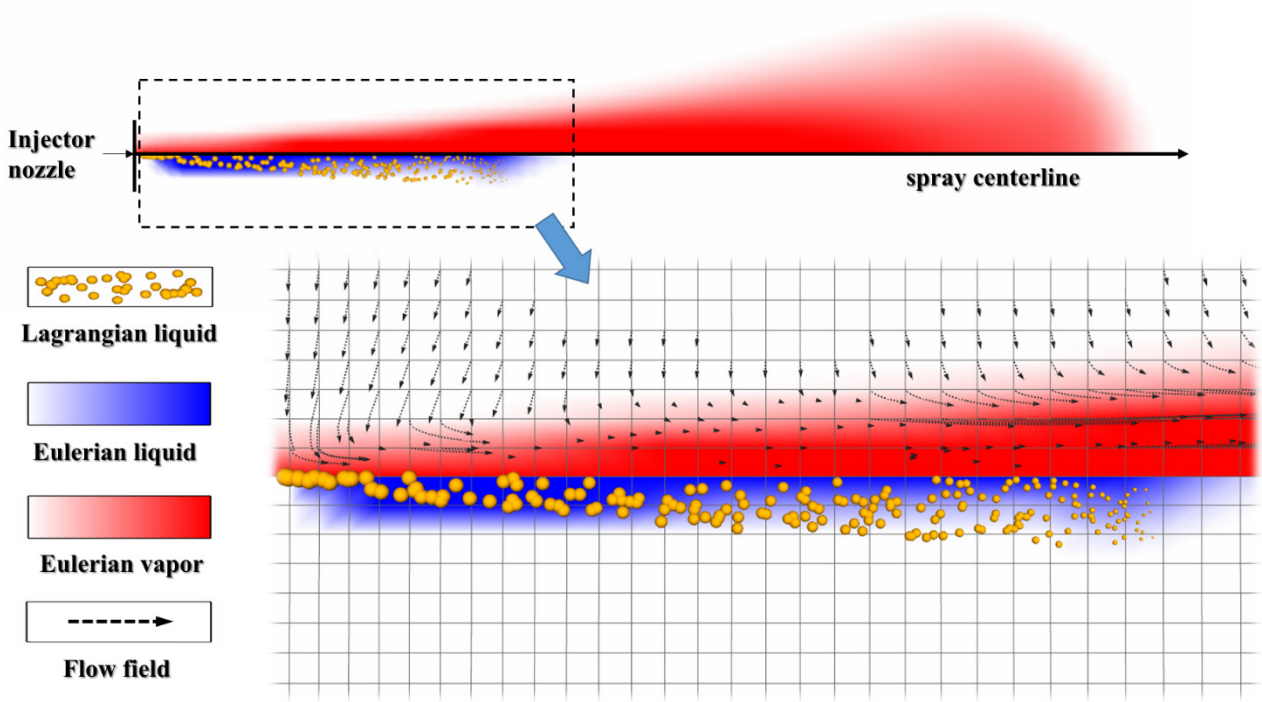

Yue, 2017

Equilibrium Phase (EP) spray model

- In the EP model the liquid is injected into the computational domain as Lagrangian parcels, as in the LDEF approach, then released to the Eulerian liquid phase

$$\text{Lagrangian liquid} \xrightarrow{\text{release}} \text{Eulerian liquid} \xleftrightarrow{\text{local equilibrium}} \text{Eulerian vapor}$$

- The Eulerian liquid phase is assumed to be perfectly mixed with the local gaseous phase, and is governed by the transport equation,

$$\frac{\partial \rho_l}{\partial t} + \nabla \cdot (\rho_l \mathbf{u}) = \nabla \cdot \left[\rho_a D \nabla \left(\frac{\rho_l}{\rho_a}\right)\right] + \dot{S}_{EP} + \dot{S}_{release} \qquad (6)$$

Phase Equilibrium Solver

Liquid-Jet model

$$\dot{S}_{release} = \left(m_{parcel} - m_{parcel,initial} \cdot (1 - \gamma(x))\right)/dt$$

$$\gamma(x) = \frac{\dot{m}_a(x)}{\dot{m}_a(L)} = \frac{\sqrt{1+16\tilde{x}^2}-1}{\sqrt{1+16(L/x^+)^2}-1} \qquad (7)$$

Yue, 2017

Phase Equilibrium Solver

Step 1: Phase stability test (Tangent Plane Distance)

Step 2: Phase split calculation (Rachford-Rice algorithm)

- ✓ The phase equilibrium solver is capable of capturing the distinctive phase behavior of a pure species and a mixture
- ✓ Purely dependent on thermodynamic states and the employed Equation of State;

Qiu, 2014

Phase diagram of binary nC16H34 and iC8H18 mixtures. Stars represent the critical point of the pure species. Phase regions are marked for a mixture with 30:70 (mole) composition. "V" stands for the vapor phase, "L" stands for the liquid phase and "L+V" stands for the vapor-liquid two-phase region.

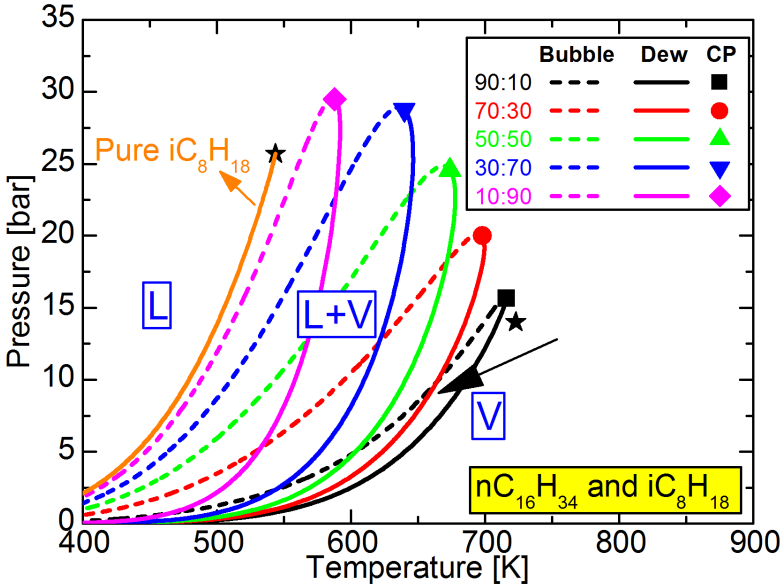

Yue, 2017

Peng-Robinson Equation of State (PR EoS)

$$P = R_u T/(\bar{v} - b) - a/(\bar{v}^2 + 2b\bar{v} - b^2)$$

$$\begin{cases} a = 0.45724\, R_u{}^2 T_c{}^2/P_c{}^2 \left[1 + f(\omega)(1 - \sqrt{T_c/T})\right]^2 \\ b = 0.07780\, R_u T_c/P_c \end{cases}$$

Van der Waals mixing rule:

$$a_m = \sum_i \sum_j x_i x_j (a_i a_j)^{\frac{1}{2}} (1 - k_{ij});$$
$$b_m = \sum_i x_i b_i$$

Species for EoS calculations

Species	$nC_{12}H_{26}$	iC_8H_{18}	nC_7H_{16}	N_2	O_2	CO	CO_2	H_2O
T_c [K]	658.0	543.8	540.2	126.2	154.6	132.92	304.19	647.13
P_c [bar]	18.2	25.7	27.4	33.9	50.43	34.99	73.82	220.55
ω[-]	0.5764	0.3034	0.3495	0.0377	0.0222	0.0663	0.2276	0.3449

Yue, 2017

Other Improved CFD Models

- Generalized Renormalization Group (gRNG) k-ε model

  Wang, 2011

  ✓Accounts for flow compressibility and has model coefficients that are functions of flow strain rate.

  ✓Improved predictions for compression flows of interest in engines
- SpeedChem

  Perini, 2012

  ✓Analytical Jacobian approach with the sparse LSODES solver

  ✓Tabulation with a fourth-degree interpolation for temperature-dependent thermodynamics properties calculation
- Chemistry mechanism

  Wang, 2013, 2014, 2015

  ✓n-heptane: 109 species, 543 reactions

  ✓n-dodecane: 100 species, 432 reactions

  ✓NOx: 4 species, 12 reactions

  ✓Polycyclis Aromatic Hydrocarbon (PAH): A1~A4
- Semi-detailed soot model

  Vishwanathan, 2011

  ✓Soot inception through A4

  ✓Surface growth through C_2H_2 and PAH

  ✓Oxygen oxidation (Nagle and Strickland-Constable model)

  ✓OH oxidation (Fenimore and Jones model)

Yue, 2017

ECN Spray A modeling

	Case #	Nominal temp. [K]	Nominal density [kg/m3]	O_2 [% vol.]	Nozzle diameter [μm]	Cd [-]	Inj. Duration [ms]	Inj. Pressure [MPa]
Spray A	1	900	22.8	0	84	0.89	6	150
	2	1100	15.2	0				
	3	850	22.8	15	91			
	4	900	22.8	13				
	5	900	22.8	15				
	6	900	22.8	21				
	7	1000	22.8	15				

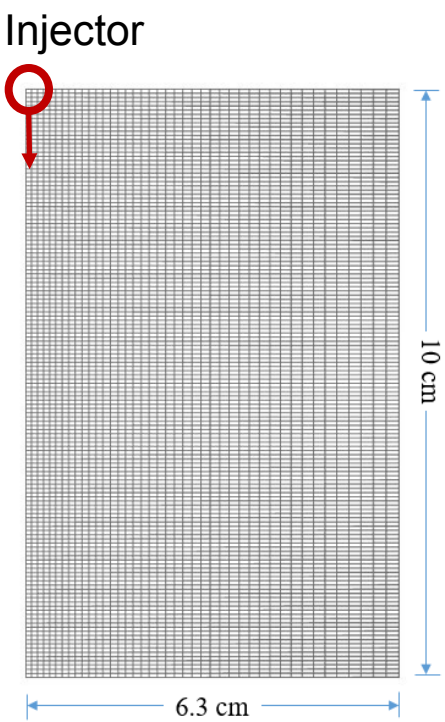

- 0.5 degree sector mesh;
- 0.7 mm * 0.7 mm
- The boundary wall is assumed black and at temperature of 450 K

Yue, 2017

ECN Spray A modeling

case 1: 900K, 22.8 kg/m, 0% O_2

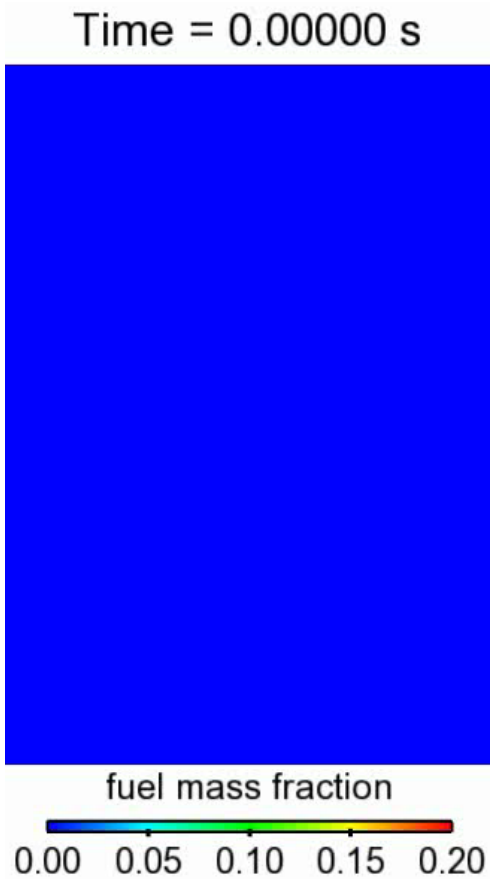

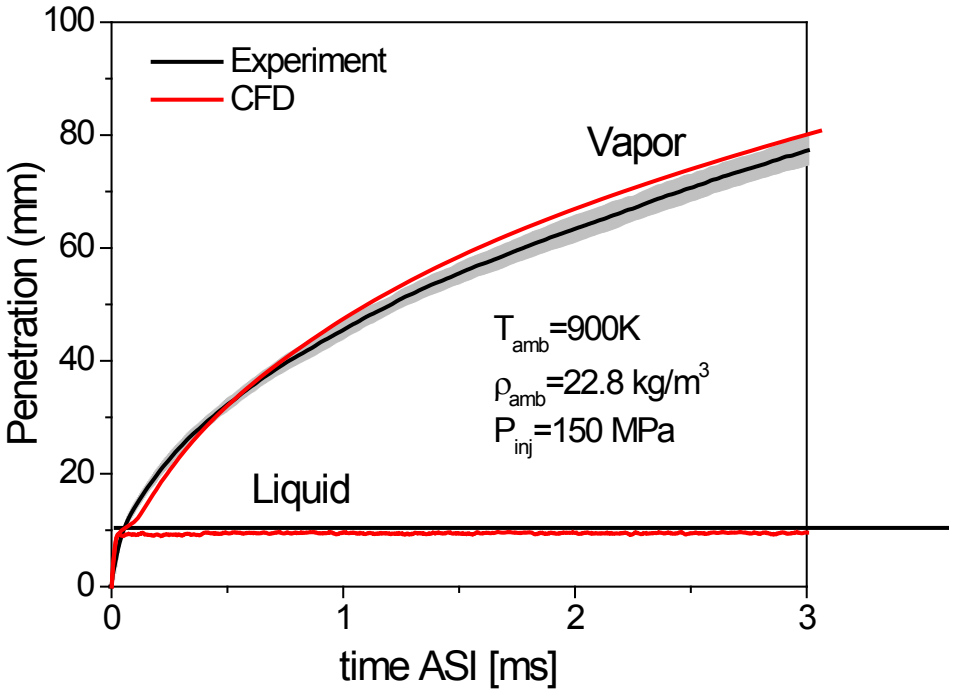

Vapor and liquid penetration for case 1

Yue, 2017

ECN Spray A modeling

Quasi-steady state fuel mixture fraction at different locations for case 1 - 900K, 22.8 kg/m, 0% O_2

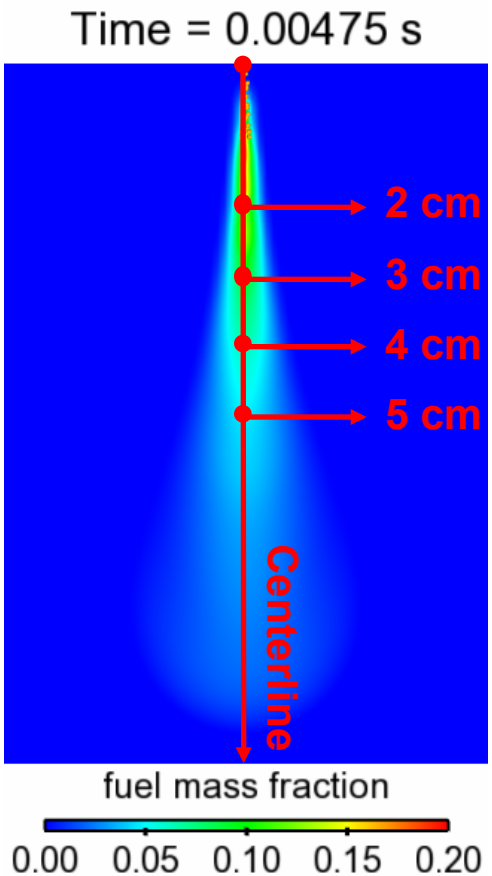

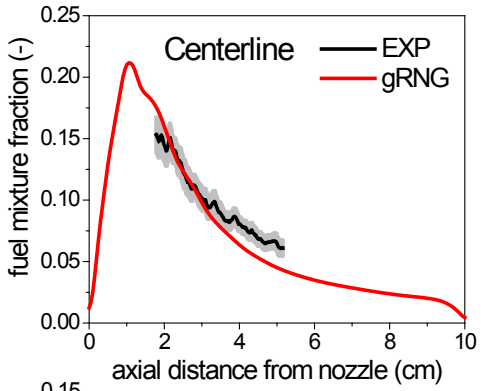

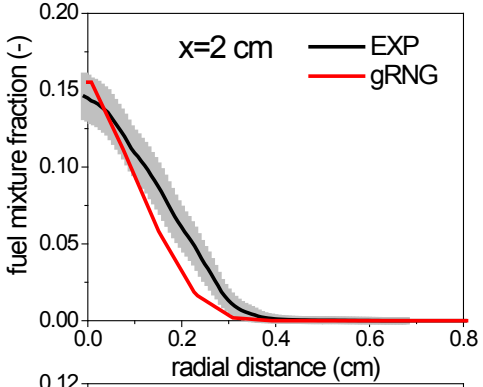

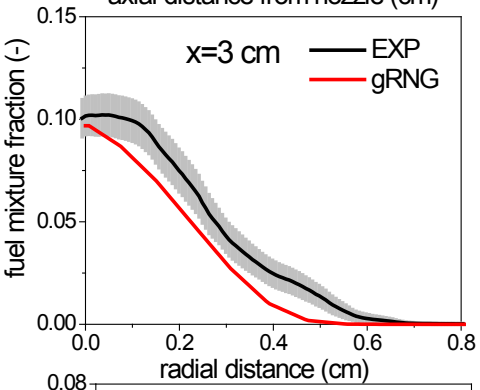

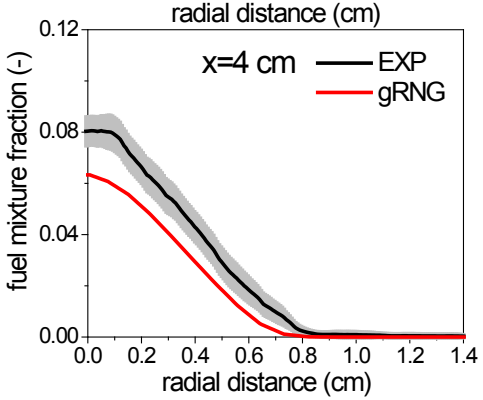

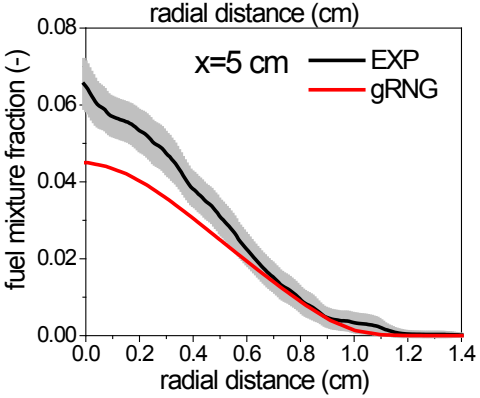

Yue, 2017

ECN Spray A soot modeling

Case3~7

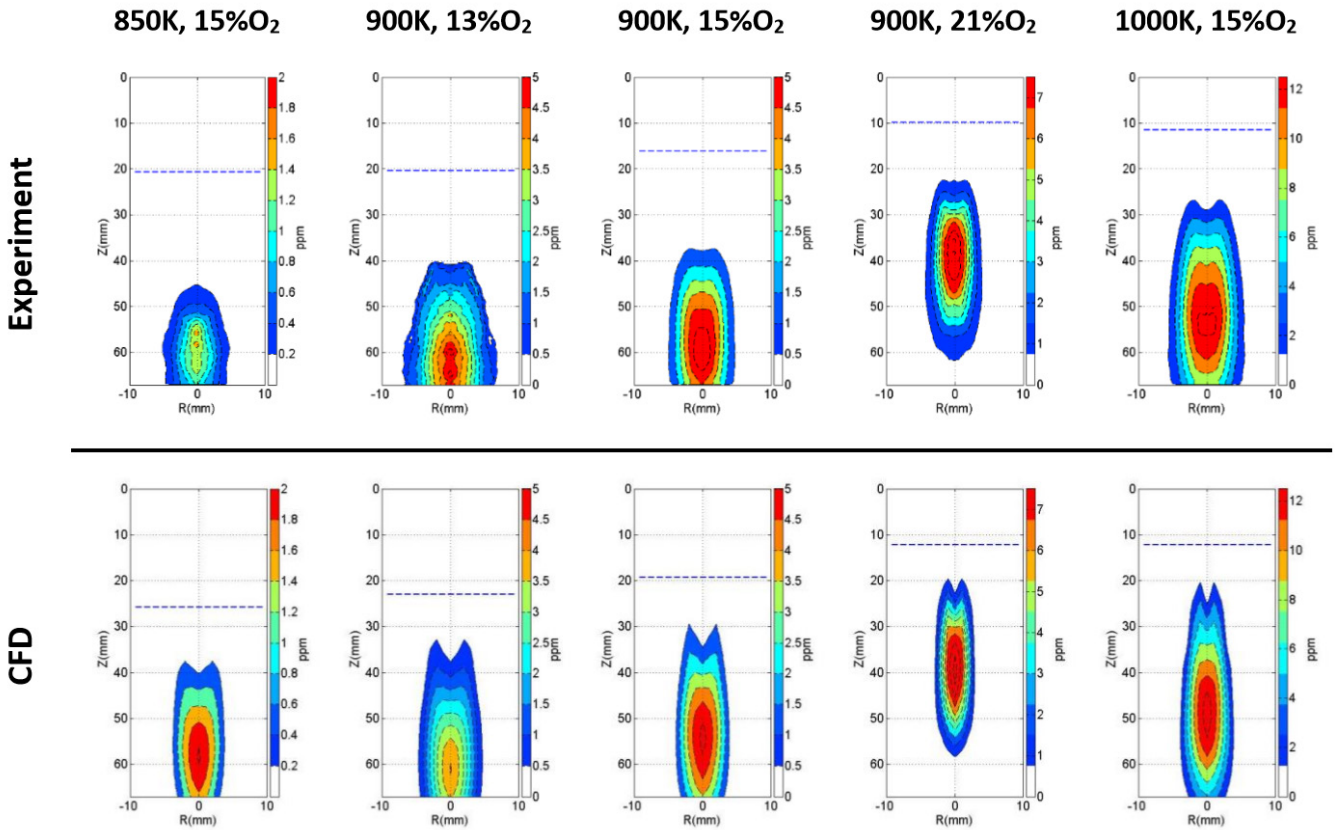

Quasi-steady state soot volume fraction (contour) and lift-off length (blue dashed line)

Diesel sprays can be modeled as an equilibrium process!

Jiao, 2015

Modeling of spray drop processes still needed for low pressure sprays and cold-start applications

- **Start of injecting timing**

CA	SOI = -330 ATDC	SOI = -320 ATDC	SOI = -290 ATDC
10^0 after SOI	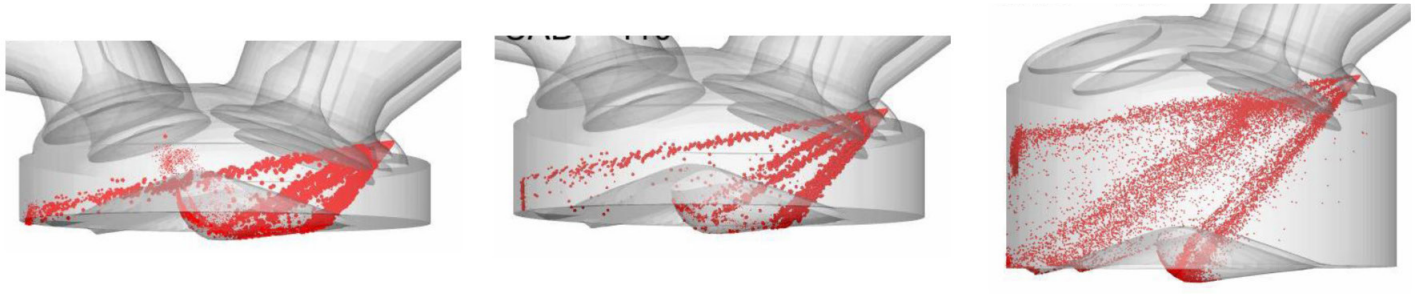		
20^0 after SOI	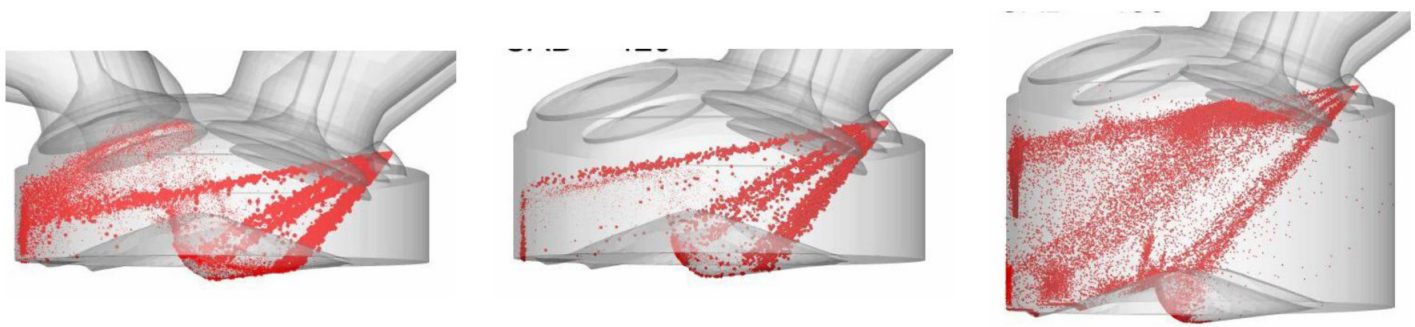		
-10^0 ATDC	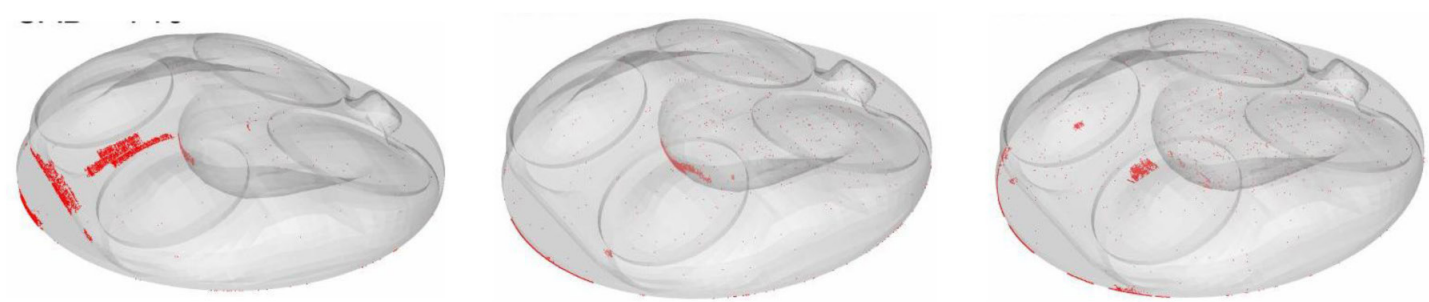		

Tan, 2004
Reitz, 2009

Summary

CFD modeling can describe both diesel and spark-ignition combustion characteristics over a wide range of conditions.

Diesel (mixing-controlled) and premixed combustion is adequately represented without requiring modeling of sub-grid-scale turbulence-chemistry interactions.

The effect of turbulence on combustion is modeled satisfactorily using an integrated G-equation-based combustion model with detailed chemical kinetics (CHEMKIN).

The G-equation-CHEMKIN model allows all combustion regimes to be modeled (**GAMUT**: G-equation for All Mixtures – a Universal Turbulent combustion model – Tan & Reitz, 2004, Reitz & Sun, 2009).

High pressure diesel sprays can be modeled as an equilibrium process! Sub-processes (atomization, drop breakup, collision/coalescence, vaporization) do not need to be modeled in EP model!

More research is needed to determine when Equilibrium Phase modeling can be safely applied.

References

3-8:4 Kalghatgi, G. Is it really the end of internal combustion engines and petroleum in transport? Applied Energy (In Press), 2018

3-8:6,7,9,11,13 Singh, S., Musculus, M.P.B., and Reitz, R.D., "Mixing and Flame Structures Inferred from OH-PLIF for Conventional and Low-Temperature Diesel Combustion", Combustion and Flame, vol. 156, no. 10, pp. 1898–1908, 2009.

3-8:8-16 Kokjohn, S.L., and Reitz, R.D., "Investigation of the Roles of Flame Propagation, Turbulent Mixing, and Volumetric Heat Release in Conventional and Low Temperature Diesel Combustion," ASME J. Eng. Gas Turbines Power, Vol. 133, pp. 102805-1-10, 2011.

3-8:17,19-27 Yue, Z., and Reitz, R.D., "An equilibrium phase spray model for high-pressure fuel injection and engine combustion simulations," IJER, DOI: 10.1177/1468087417744144, 2017.

3-8:17,18 Siebers, D.L., “Liquid-Phase Fuel Penetration in Diesel Sprays,” SAE 980809, 1998.

3-8:21 Qiu, L., Wang, Y., and Reitz, R.D., "On regular and retrograde condensation in multiphase compressible flows, ," International Journal of Multiphase Flow, Vol. 64, pp. 85-96. http://dx.doi.org/10.1016/j.ijmultiphaseflow.2014.05.004, 2014.

Slide 3-8:23

Wang, B.-L., et al., 2011, SAE Technical Paper 2011-01-0829.

Perini, F., et al., 2012, Energy and Fuels, Vol. 26, pp. 4804–4822.

Wang, H., et al., 2015, Combustion and Flame, Vol. 162, pp. 2390–2404.

Wang, H., et al., 2014, Fuel, Vol. 136, pp. 25–36.

Wang, H., et al., 2013, Combustion and Flame, Vol. 160 (3), pp. 504-519.

Vishwanathan, G., 2011, PhD thesis, University of Wisconsin, Madison.

References

3-8:28 Jiao, Q., and Reitz, R.D., "The Effect of Operating Parameters on Soot Emissions in GDI Engines," SAE Int. J. Engines 8(3):2015, doi: 10.4271/2015-01-1071, 2015.

3-8:29 Tan, Z., and Reitz, R.D., “Development of a Universal Turbulent Combustion Model for Premixed and Direct Injection Spark/Compression Ignition Engines,” SAE Paper 2004-01-0102, 2004.

3-8:29 Reitz, R.D., and Sun, Y., "Advanced computational fluid dynamics modeling of direct injection engines," in Advanced direct injection combustion engine technologies and development, Vol. 2 (18), 676-707, Woodhead, 2009.